

Silica-Pillared H-kenyates: Interlamellar Base Catalyzed-Reaction of Tetraethylorthosilicate in Water Suspension

Oh-Yun Kwon* and Sang-Won Choi

Department of Chemical Engineering, Yosu National University, Yosu, Jeon-Nam 550-749, Korea

Received August 19, 1998

The silica-pillared H-kenyates were prepared by interlamellar base-catalyzed reaction of tetraethylorthosilicate [TEOS, $\text{Si}(\text{OC}_2\text{H}_5)_4$] intercalated into the interlayer of H-kenyate. The intercalation of TEOS was conducted by the octylamine preswelling process, resulting in a dramatic increase in gallery height to 24.7 Å. The interlamellar hydrolysis of octylamine-TEOS/H-kenyate paste were conducted between 10 min and 40 min in 0.00%, 0.05% and 0.10% NH_3 -water solution respectively, and resulting in siloxane-pillared H-kenyate with gallery height of 28.2–31.8 Å. The calcination of samples at 538 °C resulted in silica-pillared H-kenyates with a large surface areas between 411 m^2/g and 885 m^2/g , depending on the aging time and NH_3 concentration. Samples with optimum specific surface areas and well ordered-basal spacing were obtained by reaction between 10 min and 40 min in pure water and 0.05% NH_3 -water solution. Mesoporous samples with narrow pore size distribution were also prepared by reaction for 10–40 min in 0.05% NH_3 solution. Rapid interlamellar reaction of TEOS in pure water showed that intercalated octylamine itself could act as a base catalyst during interlamellar polycondensation of TEOS.

Introduction

Layered silicates such as makatite, magadiite and kenyaite have attracted interest due to their catalytic, adsorptive and ion-exchange properties.¹ In recent years, silica-pillaring into the interlayer of these materials has been introduced by a few researchers.^{2–11} The pillaring procedures developed for the smectite clay are not generally applicable to the wide variety of laminar metal oxides that do not spontaneously delaminate in water.

Recently, Landis *et al.*² found that the pillaring could be facilitated by utilizing a preswelling step in which the interlayer is exposed to organoammonium ion or amine and a partial exchange of interlayer octylamine by TEOS. Daily and Pinnavaia³ synthesized supergallery derivatives from TEOS intercalation accompanied by preswelling procedures of H-magadiite. They derived interlamellar hydrolysis of TEOS in pure EtOH suspension. In the sol-gel process, a solvent such as EtOH was added to prevent the liquid-liquid separation during the initial stage of the hydrolysis reaction and to control the concentration of precursor species and water that influenced the gelation kinetics.¹² The hydrolysis reaction of TEOS by the pure EtOH suspension occurs very slowly due to the shortage of water, which may be required in interlamellar hydrolysis of TEOS. Therefore, TEOS can be released outside the layered phase during a long hydrolysis because it dissolves well in EtOH, bringing on the formation of extra-gallery silica.

Jeong *et al.*^{9,11} showed that the acid- or base-catalyzed interlamellar polycondensation of TEOS in EtOH-water suspension could minimize the formation of extra-gallery silica. Recently, Pinnavaia *et al.*¹³ also reported that the TEOS intercalated clay could be obtained easily by applying

amines as an additional swelling agent to the Li^+ -fluorohectorite clay ion-exchanged with quaternary-ammonium cations, with base-catalyzed reaction of TEOS resulting in supergallery derivatives. They suggested that the interlamellar quaternary-ammonium and co-template amines could act as micelle templates during the polycondensation of TEOS within the gallery of an ionic lamellar solid.

We report that the base-catalyzed interlamellar hydrolysis of TEOS in water without alcohol is quite effective in the preparation of silica-pillared molecular sieves from layered silicates. Also, we show that the octylamine in intersurface like NH_3 can act as a base catalyst during interlamellar polycondensation of TEOS.

Experimental Section

Synthesis of Na-kenyaite and H-kenyaite. Materials used were silica gel (Wakogel, Q-63) and analytical reagent grades of NaOH, Na_2CO_3 , ammonia water and HCl. Tetraethylorthosilicate and octylamine were special grades (Aldrich, USA).

Synthetic Na-kenyaite was prepared by the reaction of NaOH/ Na_2CO_3 - SiO_2 system under hydrothermal conditions. The experiment was carried out in a stainless steel autoclave without stirring for 72 h at 170 °C under autogenous pressure, using molar ratios of $\text{SiO}_2 : \text{NaOH} : \text{Na}_2\text{CO}_3 : \text{H}_2\text{O} = 30 : 1 : 2 : 600$. The product was filtered and washed with deionized water in order to remove excess NaOH or Na_2CO_3 , and dried at 40 °C. H-kenyaite was prepared by the ion exchange of Na-kenyaite for H^+ in 0.1 N HCl solution using the method of Beneke and Lagaly.¹⁴ The suspension composed of Na-kenyaite (100 g) and deionized water (500 mL) was titrated slowly with 0.1 N HCl solution to a final

pH 1.8 and then maintained at the same value for an additional 24 h. H-kenyaite was recovered by filtering, washed with deionized water until Cl-free, and then dried in air at 40 °C.

TEOS-intercalated H-kenyaite. Air-dried H-kenyaite (0.86 g, 0.57 mmol) was reacted with excess octylamine (2.0 g, 15 mmol) for 2 h at 25 °C. During octylamine addition, H-kenyaite absorbed the liquid amine, immediately forming a gray gelatinous mixture that does not flow. The gel was suspended with stirring in a large excess TEOS (15 g, 72 mmol) for 24 h at 25 °C, and unreacted TEOS decanted after centrifugal separation. These procedures resulted in TEOS-intercalated H-kenyaite gel by the exchange of octylamine intercalated from the preswelling step for TEOS.

Interlamellar polycondensation of TEOS. Polycondensation of intercalated-TEOS was conducted in NH_3 -water solution without alcohol. NH_3 -water solutions were prepared, containing 0.00%, 0.05% and 0.10% NH_3 in deionized water. The reaction was conducted by dispersing TEOS-intercalated H-kenyaite paste in 10 mL of each NH_3 water solution with stirring at 25 °C for 10 min, 20 min and 40 min, respectively. Viscous gray gels changed to white solid after 5 min, exothermic reactions causing a bubble. Each sample of white solid was filtered at various intervals of soaking time, washed three times with EtOH, and oven dried at 90 °C. Dried powders were calcined at 538 °C for 4 h in air to remove water, amine and organic byproducts from TEOS hydrolysis. The resultant samples afforded silica-pillared H-kenyaite.

X-ray diffraction data were recorded using a Rigaku diffractometer with $\text{CuK}\alpha$ radiation. The samples of octylamine-intercalated H-kenyaite and TEOS-intercalated H-kenyaite were prepared by smearing a thin film across a microscope slide, after which recorded the diffraction patterns of the wet samples were recorded. X-ray diffraction data for the uncalcined and calcined solid samples from the interlamellar hydrolysis reaction of TEOS were recorded by the conventional procedures. Nitrogen adsorption/desorption isotherms were determined by Micromeritics ASAP 2000 at 77 K. All samples were outgassed at 300 °C under a vacuum for 4 h. The surface areas were determined by the BET equation, and the pore size distributions of silica-pillared H-kenyaite were determined by the method of Horvath and Kawazoe equation.¹⁵ The scanning electron micrographs (SEM) were obtained from a JEOL JSM-840A scanning electron microscope. Thermogravimetric analysis (TGA) were performed in air by using a Dupont 9900 thermogravimetric analyzer. All samples were heated to 900 °C at a heating rate of 10 °C/min.

Results and Discussion

Synthesis of Na-kenyaite and H-kenyaite. The hydrothermal reaction for 72 h at 170 °C in molar ratios of SiO_2 : NaOH : Na_2CO_3 : H_2O = 30 : 1 : 2 : 600 afforded well-crystallized Na-kenyaite. The X-ray powder diffraction pattern of an air-dried product shown in Figure 1a exhibits several 00l

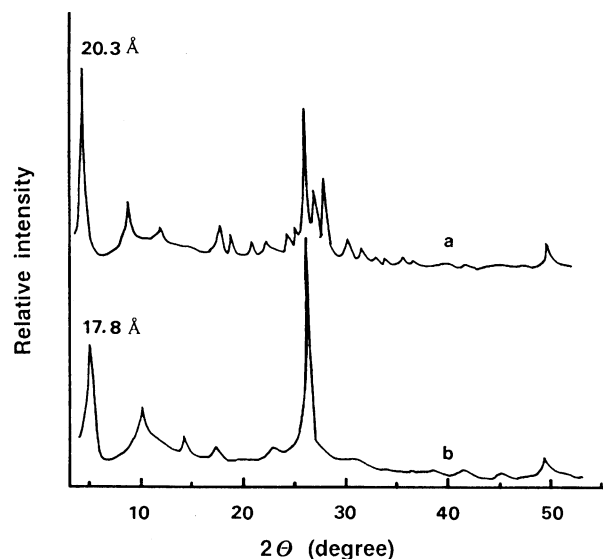


Figure 1. X-ray diffraction patterns of Na-kenyaite (a) and H-kenyaite (b).

reflections corresponding to a basal spacing of 20.3 Å. The peak positions for this synthetic product agree closely with the values reported previously.¹⁴ The slow titration of Na-kenyaite with 0.1 N HCl resulted in the exchange of sodium ions for protons in the layer structure. The X-ray powder diffraction pattern of air-dried H-kenyaite, as shown in Figure 1b, exhibited 00l reflections corresponding with a basal spacing of 17.8 Å, in agreement with earlier work.¹⁴ The decrease in basal spacing indicates a loss of interlayer H_2O .



Figure 2. The scanning electron micrographs of Na-kenyaite (a) and H-kenyaite (b).

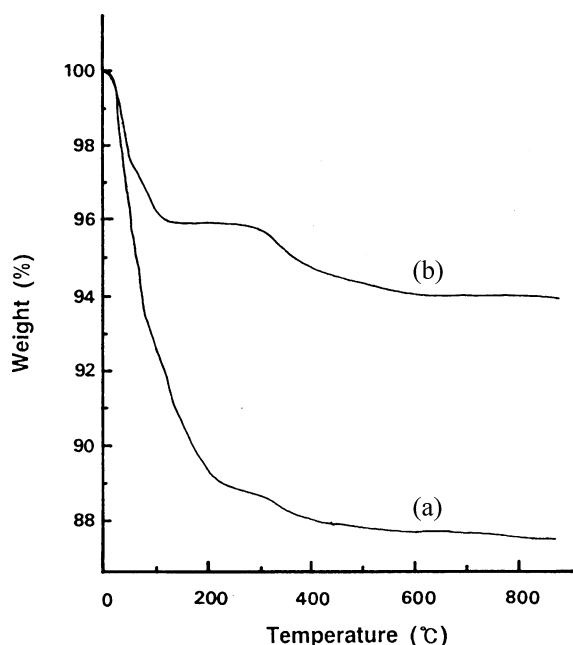


Figure 3. Thermogravimetric analysis curves of Na-kenyaite (a) and H-kenyaite (b).

upon replacement of Na^+ by H^+ . The replacement of Na^+ by H^+ in layered silicates give rise to organophilic properties in interlayer surfaces, because the silanol groups produce hydrogen bonding sites.

The scanning electron micrographs of Na-kenyaite and H-kenyaite are shown in Figure 2. Na-kenyaite shows a particle morphology composed of silicate layers intergrown to form spherical nodules resembling rosettes. H-kenyaite also exhibits the particle morphology characteristic of Na-kenyaite.

The chemical compositions of Na-kenyaite and H-kenyaite were obtained by combining the results of thermogravimetric analysis and the EDS analysis (the content of silica and sodium). The TGA data and the chemical compositions of Na-kenyaite and H-kenyaite are illustrated in Figure 3 and Table 1. As shown by the thermogravimetric curve in Figure 3a, air-dried Na-kenyaite loses 11% of its total weight as water below 300 °C. An additional 1.5% by weight is lost between 300 °C and 900 °C. The weight loss above 300 °C is attributed to the dehydration of silanol groups. By combining the composition of Na_2O (4.2 wt%), SiO_2 (83.0 wt%) and weight loss, we obtained an empirical composition for synthetic Na-kenyaite of $\text{Na}_{1.96}\text{Si}_{20}\text{O}_{40.8} \cdot 10\text{H}_2\text{O}$, which compares well with approximate composition of $\text{Na}_2\text{Si}_{20}\text{O}_{41} \cdot 10\text{H}_2\text{O}$ supported by the earlier work of Lagaly

Table 1. Composition of Synthetic Na-kenyaite and H-kenyaite

Samples	Weight percent			Total	Atomic ratio		
	Na_2O^a	SiO_2^a	H_2O		Na^a	Si^a	H_2O
Na-kenyaite	4.2	83.0	12.5	99.7	1.96	20	10.8
H-kenyaite	-	94.0	6.0	100	-	20	4.2

^aEDS data

*et al.*¹⁴ The thermal analysis of H-kenyaite, as shown by the curve in Figure 3b, indicates an initial weight loss of 4.0% below 300 °C due to the desorption of H_2O . The 2.0% weight loss above 300 °C was attributed to the elimination of OH groups from the structure. From the water loss together with the absence of sodium, we obtained an empirical unit cell composition of $\text{H}_{2.0}\text{Si}_{20}\text{O}_{41} \cdot 4\text{H}_2\text{O}$ for the H-kenyaite.

Octylamine-intercalated H-kenyaite gel. Recently, Jeong *et al.*¹¹ reported that H-kenyaite, like H-magadiite, reacted with octylamine to form ordered bilayers of alkylammonium ions and alkylamine molecules between silicate layers. In our experiment, air-dried H-kenyaite reacted directly with excess octylamine. The X-ray diffraction pattern of octylamine/H-kenyaite gel, as shown in Figure 4a, was indicative of 38.2 Å in basal spacing. Since the layer thickness of H-kenyaite was no more than the basal spacing of air-dried H-kenyaite (17.8 Å), the corresponding gallery height could be calculated to be 20.4 Å. This value is similar to the gallery height (21.5 Å) of amine-solvated H-kenyaite in the literature.¹¹ The large increase of gallery height in layered phase is reflective of the formation of lamellar bilayers of octylammonium ions and octylamine molecules between the silicate layers because the critical length of octylamine is 12.3 Å.

Reaction between octylamine-intercalated H-kenyaite and TEOS. The reaction of octylamine-intercalated H-kenyaite gel with TEOS afforded TEOS-intercalated H-kenyaite gel with well-ordered basal spacing. Figure 4b shows the X-ray diffraction pattern for TEOS-intercalated H-kenyaite gel. The product exhibits reflections corresponding to the basal

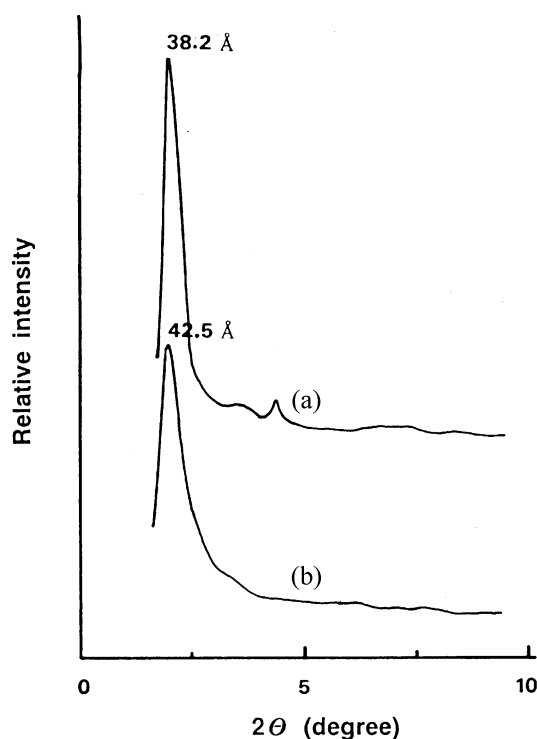


Figure 4. X-ray diffraction patterns for the octylamine-intercalated H-kenyaite gel (a) and TEOS/octylamine H-kenyaite gel (b) from solvation of interlayer octylamine by TEOS.

spacing of 42.5 (gallery height of 24.7) Å. The gallery height for the TEOS-intercalated H-kenyaite gel is about 4.3 Å larger than the gallery height (23.7 Å) of H-kenyaite gel treated with amine only. Kwon *et al.*¹⁰ showed that the gallery height of octylamine-intercalated H-magadiite could be additionally increased by introducing organic solvents. The additional increase in gallery height is attributed to the solvation of organophilic intersurface octylamine by the solvent molecules as well as the steric effect such as an arrangement and size of solvated molecules itself. During the reaction of octylamine-intercalated H-kenyaite gel with excess TEOS, TEOS could be exchanged with free amine molecules in interlayer, resulting in additional increase of gallery height. This indicates that the interlayer solvation and the bulky structure of TEOS molecules is accompanied by an increase of gallery height.

Interlamellar hydrolysis reaction of TEOS. The base-catalyzed interlamellar hydrolysis reaction of TEOS produced silica-pillared H-kenyaite with supergallery. The X-ray diffraction patterns for the uncalcined samples treated with pure water and NH_3 -water solution for 40 min at 25 °C were shown in Figure 5. The samples treated with pure water (Figure 5a) and 0.05% NH_3 (Figure 5b) exhibit well ordered-basal spacings. Actually, the interlamellar hydrolysis reaction of TEOS happens within 5 min in pure water, indicating that the interlayer amines can act as base catalysts during interlamellar hydrolysis of TEOS, because the basicity of octylamine is no less than ammonia. The octylamine may draw in the water needed in the hydrolysis of TEOS because of their water-soluble property, helping maintain a homogeneous water concentration in interlayers. This process has the advantage of preventing the outflow of TEOS from the

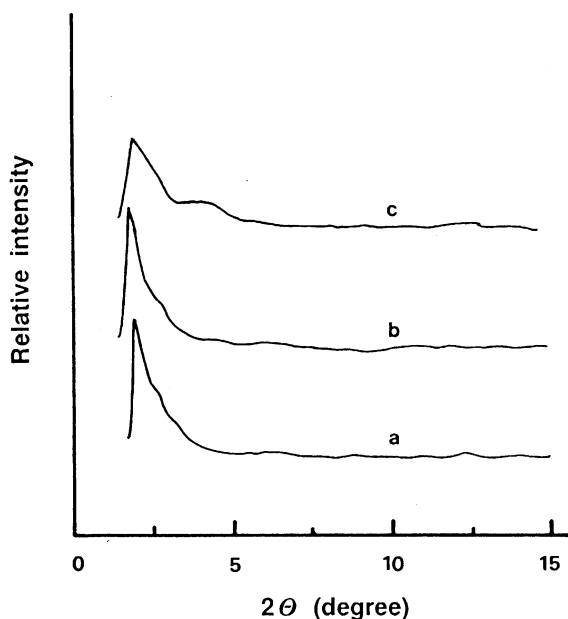


Figure 5. X-ray diffraction patterns for the uncalcined silica-pillared H-kenyaite prepared by the interlamellar hydrolysis of TEOS/octylamine H-kenyaite gel in water solution with varying NH_3 content at room temperature: a=0.00% NH_3 (pure water), b=0.05% NH_3 and c=0.10% NH_3 .

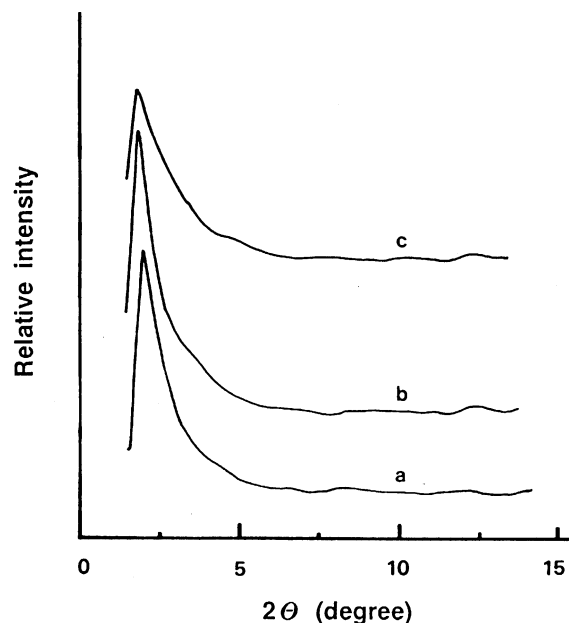


Figure 6. X-ray diffraction patterns for the calcined silica-pillared H-kenyaite prepared by the interlamellar hydrolysis of TEOS/octylamine H-kenyaite gel in water solution with varying NH_3 content at room temperature: a=0.00% NH_3 (pure water), b=0.05% NH_3 and c=0.10% NH_3 .

interlayer because TEOS is water-insoluble, and it minimize the formation of extra-gallery silica, allowing effectively silica-pillared H-kenyaite.

Figure 5b also exhibits that the silica-pillared H-kenyaite form with well-ordered basal spacing in 0.05% NH_3 . In the sol-gel process, it is known that the shapes and the formation kinetics of siloxane precursor are greatly influenced by the basicity of medium.¹⁶ The X-ray diffraction patterns in Figure 5c show, however, that the higher concentration of NH_3 results in poorly ordered-basal spacing. Figure 6 shows X-ray diffraction patterns for the calcined silica-pillared H-kenyaite. Upon removal of organic byproducts by calcination, the basal spacing decreased by 3–5, and the scattering intensity substantially increased. This suggests that the calcination process can increase the scattering contrast between the walls and the pores due to the elimination of the pore filling materials. Marler *et al.*¹⁷ reported that the intensity of X-ray peaks depend on the existence or absence of pore filling materials. Figure 7 exhibits scanning electron micrographs for the calcined silica-pillared H-kenyaite, which are aged for 10 min in 0.00%, 0.05% and 0.10% NH_3 solution. The samples treated with 0.00% NH_3 (Figure 7a) and 0.05% NH_3 solution (Figure 7b) maintained the original plate structures of H-kenyaite without broken plates or extra-gallery silica, but the sample treated with 0.1% NH_3 solution (Figure 7c) showed a severe destruction of plate structures. As the concentration of NH_3 increases from 0.00% to 0.10%, the interlamellar hydrolysis of TEOS may proceed more rapidly, and then the precursor size and shape may become larger and bulky, resulting in an increase in gallery height (Table 2). In 0.10% NH_3 and above, the gallery height may

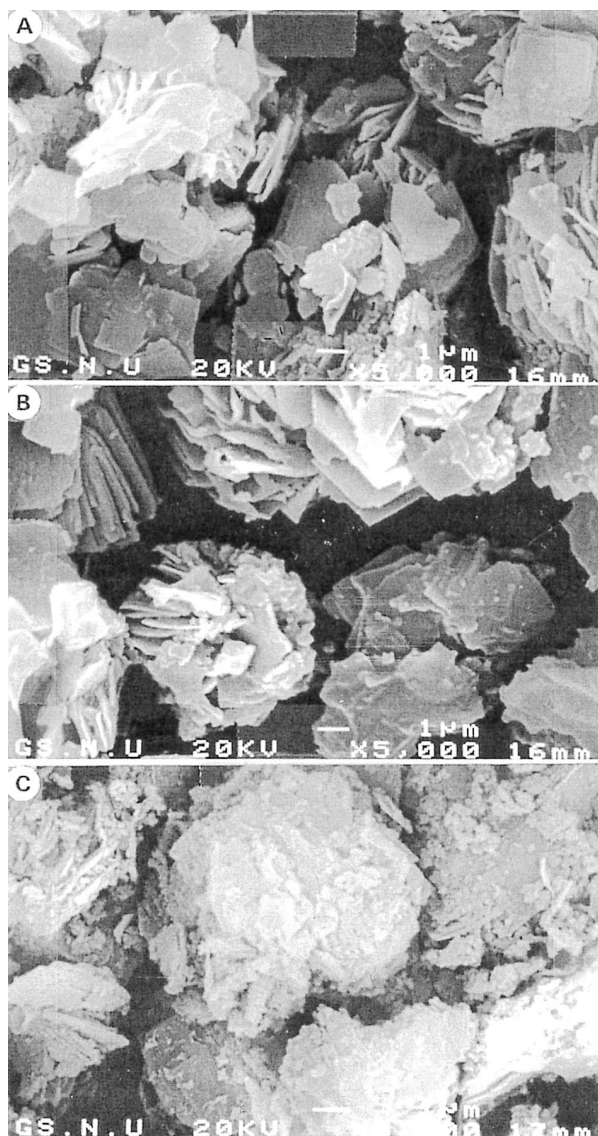


Figure 7. The scanning electron micrographs for the calcined silica-pillared H-kenyaite, hydrolyzed for 10 min in 0.00 (A), 0.05 (B) and 0.10 (C) %NH₃ solution.

be too large to maintain their structure, being replaced by nearly amorphous phase characteristics of the exfoliated siloxane composites. Figure 8 exhibits scanning electron micro graphs for the calcined silica-pillared H-kenyaite, which are produced at various aging times in 0.05% NH₃



Figure 8. The scanning electron micrographs for the calcined silica-pillared H-kenyaite, hydrolyzed for 10 (A), 20 (B) and 40 (A) min in 0.05 %NH₃ solution.

Table 2. Physical Properties of Silica-Pillared H-kenyaite Prepared at Various Aging Times and NH₃ Concentrations

NH ₃ (%)	aging time (min)	Basal spacing (Å)		Gallery height(Å)	Specific surface areas (m ² /g)
		uncalcined	calcined		
0.00	10	46.0	43.0	25.2	788
0.05	10	50.1	47.0	29.2	772
	20	51.8	48.2	30.4	740
	40	52.3	49.2	31.4	885
0.10	10	52.0	46.0	28.2	411

Gallery height=basal spacing-17.8 Å (Thickness of H-kenyaite)

solution. At varying aging times, ranging from 10 to 40 min, a partial destruction of plates happened. The increase in aging time may happen too before interlamellar polycondensation of TEOS, causing a partial collapse of layered structures. Previous results show that the basicity of medium and the aging time can be an important factor in successful preparation of silica-pillared H-kenyaite with well ordered-basal spacing from the interlamellar hydrolytic polycondensation of TEOS.

The typical nitrogen adsorption isotherms for the calcined silica-pillared H-kenyaite are shown in Figure 9. The

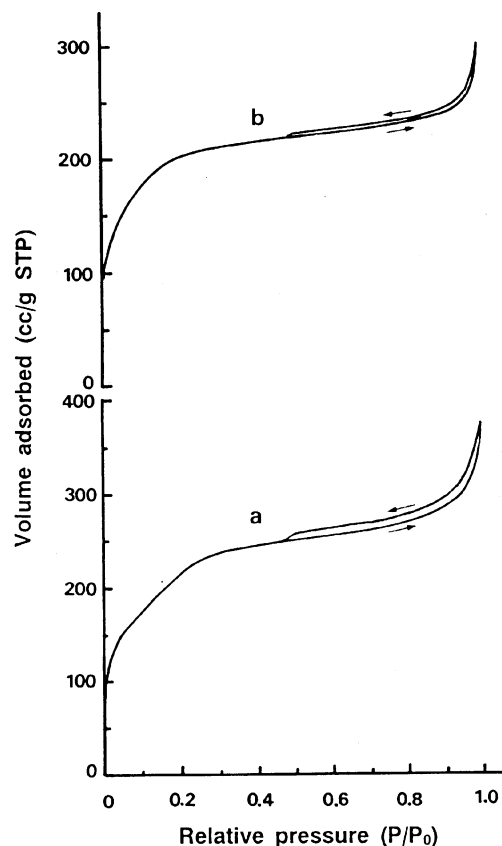


Figure 9. Nitrogen adsorption isotherms for the calcined silica-pillared H-kenyaite, hydrolyzed for 10 min in 0.05% NH_3 solution (a) and pure water (b). up-curve: adsorption, down-curve: desorption

several pore characteristics from them are listed in Table 2. The specific surface areas were calculated by BET equation from the adsorption isotherms below $P/P_0=0.1$. The specific surface areas of H-kenyaite show a low value of $76 \text{ m}^2/\text{g}$. The silica-pillared H-kenyaite, however, exhibit dramatically larger surface areas, between $411 \text{ m}^2/\text{g}$ and $885 \text{ m}^2/\text{g}$, depending on the aging time and NH_3 concentration. Most of the total surface areas are due to the presence of micropores ($< 20 \text{ \AA}$ in diameter). The gallery heights and the specific surface areas in these samples are larger than the values previously reported for the ethanol suspension.¹¹ Especially, the interlamellar hydrolysis of TEOS in pure water and 0.05% NH_3 solution resulted in a large increase in specific surface areas. This implies that interlamellar polycondensation of TEOS in pure water and lower NH_3 concentration may produce more siloxane precursor with smaller size in the galleries, controlling an outflow of TEOS from the interlayer, because TEOS is insoluble in these media and siloxane precursors cannot grow adequately over a short time. Filling up the gallery with smaller and more siloxane precursors can develop microporosity. Figure 10 shows a typical type of Horvath and Kawazoe¹⁵ pore size distribution of silica-pillared H-kenyaite. The sample prepared for 10 min in 0.05% NH_3 solution, as shown in Figure 10a, exhibits a narrow pore size distribution, resulting in a sudden

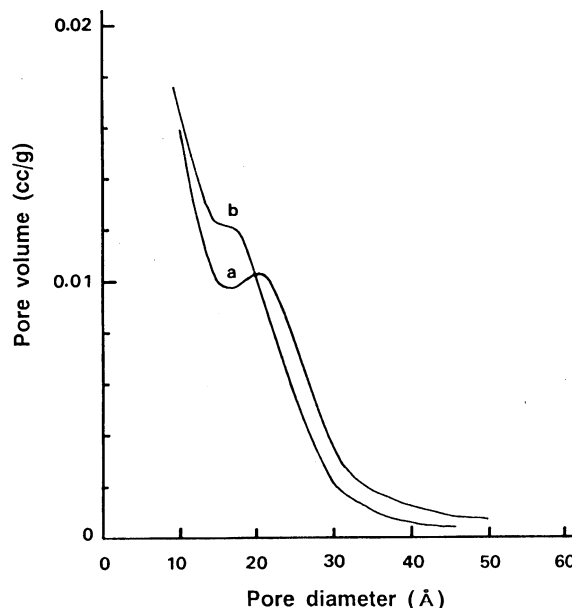


Figure 10. The pore size distributions for the calcined silica-pillared H-kenyaite, hydrolyzed for 10 min in 0.05% NH_3 solution (a) and pure water (b).

increase in mesopore volume near $\sim 22 \text{ \AA}$. This trend was observed in the samples treated for 20 min and 40 min with 0.05% NH_3 . As shown in Figure 10b, the sample treated with pure water exhibits near microporosity (diameter $< 20 \text{ \AA}$).

In particular, the silica-pillared H-kenyaite prepared by our method are very similar in physical properties to the mesoporous MCM 41.¹⁸⁻²¹ Generally, mesoporous silica-pillared layered silicates are known to have a broad pore size distribution compared with MCM 41. They, however, exhibited more acidic property and structural stability in acid-catalyzed reaction such as dehydration of 2-methyl-3-butanol with $>99\%$ selectivity.²² Because of their complementary chemical functionality and the stable pore size distribution in the micropore to small mesopore range (10–20 \AA), silica-pillared layered silicates may offer new opportunities for the rational design of heterogeneous catalyst systems.

Conclusion

TEOS-intercalated H-kenyaite with a large increase (24.7 \AA) in gallery height were prepared by octylamine pre-swelling process without pre-treating with long-chain quaternary ammonium cations. The rapid interlamellar hydrolysis of octylamine/TEOS H-kenyaite paste in pure water or 0.05% NH_3 -water solution was very effective in the preparation of silica-pillared H-kenyaite with a supergallery of 25–32 \AA . It was confirmed that the intercalated octylamine itself could act as a base catalyst during interlamellar hydrolysis of TEOS. The silica-pillared H-kenyaite exhibit dramatically larger surface areas between $411 \text{ m}^2/\text{g}$ and $885 \text{ m}^2/\text{g}$, depending on the aging time and NH_3 concentration. The scanning electron micrographs for the silica-pillared H-kenyaite show that the original plate structures are maintained

in reaction in pure water and 0.05% NH_3 solution, but severe destruction happened in reaction in 0.10% NH_3 solution. The experimental results indicate that the basicity of the medium and aging time in the medium could be important factors in controlling microporosity and mesoporous pore size distribution.

References

1. Berk, K. H.; Schweger, W.; Porsch, M. *Chem. Tech.* **1987**, 39, 508.
2. Landis, M. E.; Aufdembrink, A. B.; Chu, P.; Johnson, I. D.; Kirker, G. W.; Rubin, M. K. *J. Am. Chem. Soc.* **1991**, 113, 318.
3. Daily, J. S.; Pinnavaia, T. J.; *Chem. Mater.* **1992**, 4, 855.
4. Sprung, R.; Davis, M. E.; Kauffman, J. S.; Dybowski, C. I. *Eng. Chem. Res.* **1990**, 29, 213.
5. Yanagisawa, T.; Shimizu, T.; Kazayuki K.; Kato, C. *Bull. Chem. Soc. Jpn.* **1990**, 63, 988.
6. Yanagisawa, T.; Shimizu, T.; Kazayuki, K.; Kato, C. *Bull. Chem. Soc. Jpn.* **1989**, 61, 3743.
7. Tindwa, R. M.; Ellis, D. K.; Peng, G. Z.; Clearfield, A. J. *Chem. Soc., Faraday Trans.* **1985**, 81, 545.
8. Rituz-Hitzky E.; Rojo, J. M. *Nature* **1980**, 287, 28.
9. Jeong, S. Y.; Kwon, O. Y.; Seo, J. K.; Jin H.; Lee, J. M. *J. Colloid and Interface Sci.* **1995**, 175, 253.
10. Kwon, O. Y.; Jeong, S. Y.; Seo, J. K.; Ryu B. H.; Lee, J. M. *J. Colloid and Interface Sci.* **1996**, 177, 677.
11. Jeong, S. Y.; Seo, J. K.; Jin, H.; Lee J. M.; Kwon, O. Y. *J. Colloid and Interface Sci.* **1996**, 180, 269.
12. Brinker, C. L.; Scherer, G. W. *Sol-Gel Science: The Physics and Chemistry of Sol-Gel Processing*; Academic Press: London, **1990**; p 97.
13. Galarneau, A.; Barodawalla, A.; Pinnavaia, T. J. *Nature* **1995**, 374, 529.
14. Beneke, K.; Lagaly, G. *Am. Mineral* **1983**, 63, 818.
15. Horvath, G.; Kawazoe, K. *J. Chem. Eng. Jap.* **1983**, 16, 470.
16. (a) Aelion, R.; Loebel, A.; Eirich, F. *J. Am. Chem. Soc.* **1950**, 72, 5705. (b) Marler, B.; Oberhagemann, U.; Vortmann, S.; Gies, H. *Microporous mater.* **1996**, 6, 375.
17. Kresge, C. T.; Leonowicz, M. E.; Roth, W. T.; Vartuli, J. C.; Beck, J. S. *Nature* **1992**, 359, 710.
18. Beck, J. S.; Varturi, J. C.; Roth, W. J.; Leonowicz, M. E.; Kresge, C. T.; Schmitt, K. D.; Chu, C. T.; Olson, D. H.; Sheppard, E. W.; McCullen, S. B.; Higgins, J. B.; Schlenker, J. L. *J. Am. Chem. Soc.* **1992**, 114, 10834.
19. Tanev, P. T.; Chibwe M.; Pinnavaia, T. J. *Nature* **1994**, 368, 321.
20. Bagshaw, S. A.; Prouzet, E.; Pinnavaia, T. J. *Science* **1995**, 269, 1242.
21. Petrovic, I.; Novrotsky, A.; Chen, C. Y.; Davis, M. E. *Stud. Surf. Sci. Cata.* **1994**, 84, 677.